



NETWORK RESILIENCE FORMULATION AND RESILIENCE ENHANCEMENT DEMONSTRATION

Deliverable ID:	D3.2
Dissemination Level:	PU
Project Acronym:	START
Grant:	893204
Call:	Call: H2020-SESAR-2019-2
Topic:	SESAR-ER4-15-2019-Increased Levels of Automation for the ATM Network
Consortium Coordinator:	UC3M
Edition date:	25 May2021
Edition:	00.01.00
Template Edition:	02.00.02

Founding Members



Authoring & Approval

Authors of the document

Name/Beneficiary	Position/Title	Date
Emre Koyuncu (ITU)	WP3 leader	16/05/2021
Arinc Tutku Altun (ITU)	WP3 contributor	16/05/2021

Reviewers internal to the project

Name/Beneficiary	Position/Title	Date
Andrés Muñoz (BGD)	WP2 leader	16/05/2021
Emre Koyuncu (ITU)	WP3 leader	16/05/2021
Daniel Delahaye (ENAC)	WP4 leader	16/05/2021
Raimund Zopp (FLIGHTKEYS)	WP5 leader	16/05/2021
Alexander Kuenz (DLR)	WP6 leader	16/05/2021
Xavier Prats (UPC)	Task 2.1 and 4.1 Leader	16/05/2021

Approved for submission to the SJU By - Representatives of beneficiaries involved in the project

Name/Beneficiary	Position/Title	Date
Manuel Soler (UC3M)	Project Coordinator	25/05/2021
Andrés Muñoz (BGD)	WP2 leader	21/05/2021
Emre Koyuncu (ITU)	WP3 leader	21/05/2021
Daniel Delahaye (ENAC)	WP4 leader	21/05/2021
Raimund Zopp (FLIGHTKEYS)	WP5 leader	21/05/2021
Alexander Kuenz (DLR)	WP6 leader	21/05/2021
Xavier Prats (UPC)	Task 2.1 and 4.1 Leader	21/05/2021

Rejected By - Representatives of beneficiaries involved in the project

Name/Beneficiary	Position/Title	Date
------------------	----------------	------

Document History

Edition	Date	Status	Author	Justification
00.00.01	18/04/2021	Initial Draft	Emre Koyuncu	New document
00.00.02	30/04/2021	Complete Draft	Arinc Tutku Altun	Sent for internal review
00.00.03	14/05/2021	Complete Draft	Emre Koyuncu	Sent for internal review
00.01.00	25/05/2021	Submission	Emre Koyuncu	Internally reviewed

Copyright Statement: © – 2021 –START Consortium – All rights reserved. Licensed to the SJU under NO conditions.

START

A STABLE AND RESILIENT ATM BY INTEGRATING ROBUST AIRLINE OPERATIONS INTO THE NETWORK

This Deliverable is part of a project that has received funding from the SESAR Joint Undertaking under grant agreement No 893204 under European Union's Horizon 2020 research and innovation programme.



Abstract

This document is devoted to explaining the management methodology of the ATM macro model that will enable to choose the best actions for the resiliency of the network under disruptive events. The model is based on the integration of trajectory uncertainties, which are being quantified in WP2; disruptive events taken as input, and approximate model through the epidemic process, which has been studied in WP3. In START, at the macro level, we consider only thunderstorms, as they are more frequent and observable than the other events that impact the airports.

In this document, first, we provide the summary of the network model, then give the resiliency definition, which is connected with the stability of the network. From the operational point of view, resiliency is connected with over-treatment (high resilience) and the management cost as a function of the rate of intervention. The problem, at this point, transformed into an optimization-based control problem to ensure convergence by time, meaning the effect of disruptive events dies out eventually. Finally, the introduced optimization problem asymptotically bounded by a rate of intervention is solved through reinforcement learning methodology, providing the best actions. This intervention gives the target OD pair and number of flights requires regulation action. The case studies and results are given for the selected time windows chosen in the interval of 1-10 June of 2018, where thunderstorms affected large areas of North-West Europe with intense local convective activities.

Table of Contents

Abstract	3
Executive Summary	8
1 Introduction	9
1.1 START Project Goals.....	9
1.2 START Work Plan	10
1.3 Scope of the deliverable within START project.....	12
1.4 Acronyms	13
2 ATM Network Uncertainty Model.....	15
2.1 Model Building	15
2.2 Validation Results.....	20
3 Network Stability and Resiliency.....	25
3.1 Network Stability.....	25
3.2 ATM Network Resilience.....	26
4 RL-based Network Resilience Management	28
4.1 Proximal Policy Optimization (PPO).....	28
4.2 Results of Resilience Management under Disruptive Events.....	29
5 Concluding Remarks.....	36
6 References	37

List of Tables

Table 1. Document acronyms	13
Table 2. Airports' ICAO codes in the document.....	14
Table 3. START Consortium acronyms	14
Table 4: Infection rate changes of the flights from LSZH to the some of the major airports that have connection (June 4, 2018 - 13:30 – 16:30) after applying resilience management with constraint on rate of intervention	31
Table 5: Calculated minutes of delays (total and per flight) with and without resilience management (RM) from LSZH to the some of the major airports that have connection (June 4, 2018 - 13:30 – 16:30)	31
Table 6: Infection rate changes of the flights from EDDF to the some of the major airports that have connection (June 7, 2018 - 12:30 – 15:30) after applying resilience management with constraint on rate of intervention	32
Table 7: Infection rate changes of the flights from LEBL to the some of the major airports that have connection (June 7, 2018 - 12:30 – 15:30) after applying resilience management with constraint on rate of intervention	33
Table 8: Calculated minutes of delays (total and per flight) with and without resilience management (RM) from EDDF and LEBL to the some of the major airports that have connection (June 7, 2018 - 12:30 – 15:30)	33
Table 9: Infection rate changes of the flights from EDDM to the some of the major airports that have connection (June 10, 2018 - 13:00 – 16:00) after applying resilience management with constraint on rate of intervention	34
Table 10: Infection rate changes of the flights from EDDF to the some of the major airports that have connection (June 10, 2018 - 13:00 – 16:00) after applying resilience management with constraint on rate of intervention	34
Table 11: Calculated minutes of delays (total and per flight) with and without resilience management (RM) from EDDM and EDDF to the some of the major airports that have connection (June 10, 2018 - 13:00 – 16:00)	35

List of Figures

Figure 1: START overall concept figure	10
Figure 2: Work plan breakdown.....	11
Figure 3: Airport-based metapopulation epidemic process model.....	17
Figure 4: Metamodel representation of the flow between two airports.....	17
Figure 5: DNN representation of the considered model for estimation of recovery rates.....	19
Figure 6: Recovery Rate estimation for June 2, 2018 (18:00 – 21:00).....	19
Figure 7: Recovery Rate estimation for June 3, 2018 (13:30 – 16:30).....	20
Figure 8: Recovery Rate estimation for June 7, 2018 (14:30 – 17:30).....	20
Figure 9: Comparison for evaluated fractions of the model and real fractions on June 2, 2018 (13:30 – 16:30)	21
Figure 10: Comparison for evaluated fractions using network model and real fractions on June 2, 2018 (17:30 – 20:30)	21
Figure 11: Comparison for evaluated fractions of the model and real fractions on June 3, 2018 (13:30 – 16:30)	22
Figure 12: Comparison for evaluated fractions of the model and real fractions on June 6, 2018 (17:30 – 20:30)	22
Figure 13: Comparison for evaluated fractions of the model and real fractions on June 8, 2018 (16:00 – 19:00)	23
Figure 14: Comparison for evaluated fractions of the model and real fractions on June 8, 2018 (18:00 – 21:00)	23
Figure 15: Comparison for evaluated fractions of the model and real fractions on June 9, 2018 (15:00 – 18:00)	24
Figure 16: Comparison for evaluated fractions of the model and real fractions on June 9, 2018 (18:00 – 21:00)	24
Figure 17: The bounded stability region for system eigenvalues	26
Figure 18: High resilience, mid resilience and low resilience as defined in (Gluchshenko & Foerster, 2013) – depends on settling time value, which can be controlled by $\alpha > 0$ distance, a parameter defines rate of intervene.....	26
Figure 19: Representation of reward function wrt maximize the stability and minimize the management cost	27

Figure 20. Observed disruptive events over North-West Europe in June 2018 as see in EUROCONTROL's Monthly Network Operation Report 30

Figure 21: Comparison between evaluated fractions a) without resilience management and b) after resilience management without constraint on rate of intervention (high resilience), and c) after resilience management with constraint on rate of intervention for June 4, 2018 (13:30 – 16:30) 31

Figure 22: Comparison between evaluated fractions a) without resilience management and b) after resilience management without constraint on rate of intervention (high resilience), and c) after resilience management with constraint on rate of intervention for June 7, 2018 (12:30 – 15:30) 32

Figure 23: Comparison between evaluated fractions a) without resilience management and b) after resilience management without constraint on rate of intervention (high resilience), and c) after resilience management with constraint on rate of intervention for June 10, 2018 (13:00 – 16:00) 34

Executive Summary

START proposes a framework for obtaining robust airline operations that would lead to a stable and resilient Air Traffic Management (ATM) performance in any kind of disruptive scenario by means of a combination of methods from applied mathematics. Consequently, the focus will be on providing the capabilities required to update the planned flight trajectories according to the uncertainties introduced by the disturbances in the considered air traffic scenarios, which would be a key enabler for implementing the Trajectory Based Operations (TBO) concept. For this purpose, introducing the capability of identifying potential disturbances in the system and optimizing the air traffic operations to adapt to their associated uncertainty at different operational levels was considered an essential feature of the framework.

The D3.2, the second deliverable of WP3, presents a network-level resilience management methodology of the START project based on a meta-model of the epidemic process and its control through optimization-based control. First, resilience network definition is bind to network stability through ensuring negative eigenvalues; then, the problem bounded by the number of utilized actions is transformed into a constrained optimization problem. This problem is finally solved through Proximal Policy Optimization (PPO), which is a reinforcement learning methodology. The deliverable is organized as follows:

In Section 2, the model and theoretical background are summarized, where the details were given D3.1. The validation results showing the success of the model are given.

Section 3 first provides a brief discussion on network stability and resiliency and then provides a theoretical bridge between these terms.

Section 4 explains how the resilience problem, which is converted into a well-defined optimization problem, is solved through reinforcement learning methodology. Then the results from the management implementation are given.

Section 5 provides final concluding remarks regarding the ATM network modeling and resilience management.

1 Introduction

1.1 START Project Goals

The development, implementation and validation of optimization algorithms for robust airline operations that result in stable and resilient ATM performance even in disturbed scenarios is the overall goal of START. To reach this goal, START will combine various methods from applied mathematics, i.e.: mathematical optimization, optimization under uncertainty, Artificial Intelligence (AI) and data science, as well as algorithm design. Furthermore, insight into the uncertainties relevant in TBO systems will be gained through simulations. According to START's PMP (SESAR Exploratory Research, 2020), the main focus of the project is the optimization of conventional traffic situations while considering disruptive weather events such as thunderstorms.

The main uncertainty sources considered in this project can be classified as:

1. Uncertainties at the micro-level or trajectory level, e.g., due to inaccurate wind forecasts, aircraft performance models, aircraft weight estimation, aircraft intent, and take-off times.
2. Uncertainties at the macro-level or ATM network level, e.g., due to disruptive events in the network such as thunderstorms, due to congested airspaces or airports, and due to the propagation of micro-level (trajectory level) delays over the network.

Within the main goal stated above, the following specific goals arise:

1. To model uncertainties at the micro (trajectory) level, assimilate observations (via ADSB/Radar) every 15 min. using advanced data science methods, and propagate trajectory uncertainties using assimilated models and a stochastic trajectory predictor.
2. To model uncertainties at the macro (ATM network) level, assimilate observations (satellite data for storm, and network status) every 15 min. using advanced data science methods and propagate ATM network uncertainties using the assimilated models.
3. To develop an Artificial Intelligence (AI) algorithm capable of generating a set of pan-European (i.e., considering the whole traffic over Europe) robust trajectories that make the European ATM system resilient when facing these relevant uncertainties.
4. To implement those algorithms as an advanced flight dispatching demo functionality for airspace users to obtain robust trajectories.
5. To validate these concepts through system-wide simulation procedures in order to evaluate their stability, assessing the benefits for both the airspace users and the network manager. Recommendations for the derivation of resilient TBO networks will be derived.

The overall concept underpinning the project is sketched in Figure 1. In this structure, one can identify five blocks (each of them corresponding to the five specific goals of the project), namely: Micro-Level (trajectories); Macro-level (ATM Network); Artificial Intelligence Metaheuristic Algorithm; Flight dispatching tool; Fast-Time Simulations.

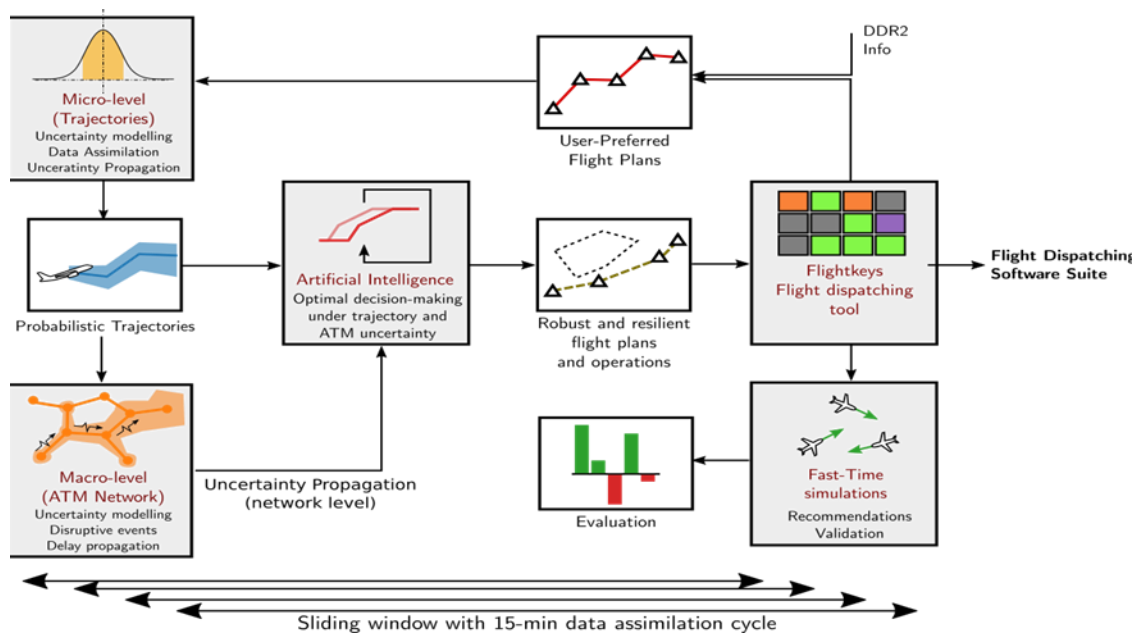


Figure 1: START overall concept figure

1.2 START Work Plan

According to START's PMP (SESAR Exploratory Research, 2020), the project is divided into seven work packages (WPs), as sketched in Figure 2, which describes the different tasks to be performed in START. The objectives of each WP are the following:

- WP1 Project management

The goal is to effectively fulfil all the administrative, contractual, financial and technical aspects of the coordination of the project.

- WP2 Trajectory level: Uncertainty modelling, data assimilation and uncertainty propagation

The goal is to develop uncertainty propagation models at trajectory level; identify and characterize potential sources of trajectory level uncertainty following a data-driven approach; build and develop methods for the cyclic ingestion of data inputs that will feed the uncertainty propagation models at the trajectory level.

- WP3 ATM Network level: network modelling, uncertainty propagation with disruptive events

The goal is to develop an approximate ATM network model from the historical data enabling to simulate and analyze uncertainty and delay propagation; integrate individual trajectory uncertainties into the network model; provide models for disruptive events and integrate them into the network-wide model; validate the model, procedures and provide a simulation environment/tool for use case analyses.

- WP4 Network-wide Robust Trajectory Planning and Resilience management based on Simulating Annealing

- WP5 Flight dispatching prototype tool

- WP6 Simulation and Validation

- WP7 Dissemination, exploitation and communication

WP1 - Management
WP7 - Communication, Dissemination, and Exploitation

WP2
 Trajectory level:
 Uncertainty modelling,
 data assimilation
 and uncertainty
 propagation

WP3
 ATM Network level:
 network modelling,
 uncertainty propagation
 with disruptive events

WP4
 Network-wide
 Robust Trajectory
 Planning and Resiliency
 Management based on
 Simulating Annealing

WP5
 Flight dispatching
 prototype tool

WP6
 Simulation and
 Validation

flight dispatching
 software suite

Sliding window with 15-min data assimilation cycle

Founding Members



1.3 Scope of the deliverable within START project

This deliverable, the second deliverable of WP3, presents a network-level resilience management methodology of the START project based on a meta-model of the epidemic process and its control through optimization-based control. First, resilience network definition is bind to network stability through ensuring negative eigenvalues; then, the problem bounded by the number of utilized actions is transformed into a constrained optimization problem. This problem is finally solved through Proximal Policy Optimization (PPO), which is a reinforcement learning methodology.

1.3.1 Literature Review

In several kinds of research, queuing network models are considered to model the air transport network system. They represent a proper perspective to analyze the impact of delay propagations over the network and response of the network to the local disturbances. Firstly, two different National Airspace System (NAS) simulation models have been developed by MITRE Corporation to simulate the delay propagation over the network that consists of nationwide airports and airspaces in the United States. The first NAS simulation model is named as National Airspace System Performance Analysis Capability (NASPAC) (Frolov & Sinnott, 1989). The second model, the Detailed Policy Assessment Tool (DPAT), which is the successor of the NASPAC (Wieland, 1997), deals with the capacity reductions on airports that may occur with disruptive external events and effects on the network of those delays when they are propagated over the system. However, DPAT does not use the information regarding the aircraft itineraries, which may cause unreliable predictions to be obtained. There are also agent-based simulation models for the delay propagation such as The Future ATM Concepts Evaluation Tool (FACET) (Bilimoria, Sridhar, Chatterji, Sheth, & Grabbe, 2001), LMINET (Long, Lee, Johnson, Gaier, & Kostiuik, 1999) and LMINET2 (Long & Hasan, Improved predictions of flight delays using LMINET2 system-wide simulation model, 2009), are national queuing network models which are using $M(t)/E_k(t)/1$ queues to model airports in the network. LMINET does not utilize aircraft itineraries while LMINET2 uses this information, which improves predictions of the simulation model. The Approximate Network Delays (AND) model is another popular model (Pyrgiotis, Malone, & Odoni, 2013) that has similarities with LMINET2 in terms of the modeling approach; however, the calculating strategies of the local queuing delays are different. Following a similar path, in our previous work, we benefit from queuing networks to model and analyze the delay characteristics of the European air traffic (Baspinar, Ure, Koyuncu, & Inalhan, 2016), and develop ground-holding policies (Bapinar, Koyuncu, & Inalhan, 2017). Then, we have further extended these studies to approximate the delay propagation dynamics of the air transportation network through the epidemic process model (Baspinar & Koyuncu, A data-driven air transportation delay propagation model using epidemic process models, 2016).

Epidemic models were mostly used to understand the dynamics of disease spreading in a network. Infection propagation between living beings were formulated by the mobility of individuals. Then the several compartment models were employed to approximate the dynamics of propagation. From a network dynamics point of view, epidemic spreading and the delay propagation methodologically very much resembles each other; local disruptive events at airports and airspaces causing retard the individual flights, and these flights spread this effect to the other airspaces and airports at specific rates. These rates are the function of certain parameters (e.g., traffic flow, flight time, etc.) subject to the interaction between the components of the network. Furthermore, control policies in the epidemic spreading such as vaccination have similarities with demand-and-capacity balancing in air transportation. These are applied through certain operational activities such as ground holdings, flight

cancellations, cruise speed decreasing/increasing. On the basis of this similarity, one can approximate the delay propagation in air transport with different types of epidemic spreading process models. In the epidemic model literature, Bernoulli is the first person that introduced the basic state model (Dietz & Heesterbeek, 2002) in the 18th century. In 1927, W. O. Kermack and A. G. McKendrick created the SIR model (Kermack & McKendrick, 1927). Compartments in this model are Susceptible (S), Infected (I) and Recovered (or Immune) (R). This was a good and simple model for many infectious diseases, including measles, mumps, and rubella. Another model was the SIS model (Zhou & Liu, 2003), (Nowzari, Preciado, & Pappas, 2016) that can be derived from the SIR model under the assumption that the individuals do not have immunity for the considered disease. These two models were also represented with vital dynamics (Hethcote, Three basic epidemiological models, 1989) that have death and birth situations. Additionally, the SIRS, SEIS, SEIR, SEIRS, MSIR and MSEIR models were also developed (Capasso & Capasso, 1993), (Hethcote, The mathematics of infectious diseases, 2000). Furthermore, the network theory (Li, van de Bovenkamp, & Van Mieghem, 2012), (Lajmanovich & Yorke, 1976) was also applied to these models to simulate the situations when infection and recovery rates are heterogeneous. Moreover, the metapopulation approach (Lajmanovich & Yorke, 1976) was also represented to model lumps of individuals as subpopulations. In several studies (Romualdo & Alessandro, 2001), (Balcan, ve diğerleri, 2009), the disease spreading in complex networks was also investigated. Besides of the modelling approaches, some control strategies were also presented to prevent the spreading of disease as quickly as possible. These were generally categorized into three: spectral control and optimization; optimal control; and heuristic feedback policies (Nowzari, Preciado, & Pappas, 2016). The idea of the spectral control based on optimization is about allocating resources optimally to hinder the spreading of disease. In this report, we focus on this approach to maximize the network resilience in air transportation against the delay spreading.

1.4 Acronyms

Non-exhaustive list of acronyms used across the text.

Table 1. Document acronyms

Acronym	Description
ATC	Air Traffic Control
ATM	Air Traffic Management
DNN	Deep Neural Network
ICAO	International Civil Aviation Organization
OD	Origin - Destination
PPO	Principle Policy Optimization
RL	Reinforcement Learning
SIR	Susceptible – Infected – Recovered
SIS	Susceptible – Infected – Susceptible
TRPO	Trust Region Policy Optimization

Table 2. Airports' ICAO codes in the document

Acronym	Description
EHAM	Amsterdam Airport Schiphol
LEBL	Barcelona El Prat Airport
EDDF	Frankfurt Airport
LTBA	Istanbul Atatürk Airport
LPPT	Lisbon Portela Airport
EGLL	London Heathrow Airport
LEMD	Madrid Barajas Airport
EDDM	Munich Airport
LFPG	Paris Charles de Gaulle Airport
LFPO	Paris Orly Airport
LIRF	Rome–Fiumicino International Airport
LSZH	Zurich Airport

START Consortium

Table 3. START Consortium acronyms

Acronym	Description
BDG	Boeing Research and Technology Europe-Germany
DLR	German Aerospace Center
ENAC	École Nationale de l'Aviation Civile
FLIGHTKEYS	FlightKeys
ITU	Istanbul Teknik Universitesi
UC3M	Universidad Carlos III de Madrid
UPC	Universitat Politècnica de Catalunya

2 ATM Network Uncertainty Model

In this section, the formulation of theoretical background of the large-scale network modeling, which is used in START Project, is summarized, enabling to simulate, analyze and control delay and uncertainty propagation in the air transport network. The details were already given in D3.1.

2.1 Model Building

The model uses Information propagation formulation over large-scale networks enable to model diffusion of information, which is quite similar to epidemic spreading. In the START project, we have chosen to follow this approach, where the ATM delay/uncertainty propagation model is based on the theory behind the epidemic/information spreading, but tailor and improve it by considering realism of ATM networks.

For the ATM Network model, have chosen the SIS compartment approach named as the Susceptible-Infected-Susceptible (*SIS*) population model where the Susceptible state stands for the individuals that are healthy and not affected (yet) but have a possibility to be infected and the Infected state represents the individuals that are affected by the spreading but able to be recovered. In the *SIS* model full recovery is not possible thus the recovered individuals turn back into the *S* state and they are open to get infected again into the state *I*. Transitions between the states within the model are ensured through specific rates such as recovery rates (δ) and infection rates (β). Both the meaning and the use case of those rates can vary depending on the epidemic model that is used. Basically, in the *SIS* model, individuals that take place in the *S* compartment become infected with β and an individual that is in *I* state recovers and turns into *S* with δ . The delay and uncertainty propagation between airports in an air transportation network has similar dynamics in terms of epidemic spreading. A local disturbance that has occurred in an airport may cause delay/uncertainty in that specific airport, which can be named as infection. That generated delay is carried by flights within the air traffic network to spread the delay/infection. Furthermore, control strategies in the epidemic spreading such as vaccination, resemble with protection strategies in the air transportation to prevent the delay propagation such as ground holdings, flight cancellations, cruise speed increasing etc.

For the mathematical model of the epidemic spreading, the evaluation of the states can be modeled as a Markov process. If the population that we are dealing with is considered as a well-mixed population (each individual can affect everyone and can be affected by everyone within the population), the infection and recovery rates hold for everyone and can be used for the dynamics of each individual. Based on that information, the following differential equations can be given for modeling the dynamics of the *SIS* model:

$$\dot{p}_{inf}(t) = \beta p_{inf}(t) p_{sus}(t) - \delta p_{inf}(t)$$

$$\dot{p}_{sus}(t) = -\beta p_{inf}(t) p_{sus}(t) + \delta p_{inf}(t)$$

where p_{inf} and p_{sus} refers to probability of being infected and probability of being susceptible, respectively. If we assume $N \in \mathbb{R}$ be the total number of individuals within the considered population and N_{inf} , $N_{sus} \subseteq N$ number of people who are infected and susceptible; p_{inf} and p_{sus} can be represented as $p_{inf} = N_{inf}(t)/N$ and $p_{sus} = N_{sus}(t)/N = (N - N_{inf}(t))/N$. It is also known that

the equality $p_{sus}(t) = 1 - p_{inf}(t)$ holds. Therefore, the dynamics of the system can be rewritten as follows:

$$\dot{p}_{inf}(t) = \beta p_{inf}(t) (1 - p_{inf}(t)) - \delta p_{inf}(t)$$

This deterministic equation is derived by assuming that the equation can be solved analytically and N is a number of individuals that is large enough to show the complete dynamics of the population. But, if the population is not large enough, behaviors of the individuals may differ depending on how large the population (N) is.

For the network model, continuous-time Markov process as a directed graph with state transitions can be considered. Let a weighted, directed graph be defined as $G = (V, E, W)$, where $V = \{v_1, \dots, v_n\}$ represents the individuals within the population which refer to set of nodes on graph G , $E \subseteq V \times V$ depicts the set of directed edges that shows connectivity between the nodes, and $W : E \rightarrow R$ is a function that assigns weights (which can be represented with infection rates in an epidemic model) to the edges in E . Assume that the node j affects the node i , then the $\beta_{ij} > 0$. If the node i and node j is not connected, then the $\beta_{ij} = 0$. Additionally, every node i has a recovery rate δ_i . The following differential equation can be considered for the network model of the SIS model:

$$\dot{p}_i(t) = -\delta_i p_i(t) + \sum_{j=1}^N \beta_{ij} p_j(t) (1 - p_i(t))$$

where the probability of being infected of the node i is given as $p_i(t) \in [0, 1]$ at any time t .

In a network system, individuals (N) can be modeled as sub-populations (M) under specific assumptions for the simplicity. In other words, instead of working on each individual within the population, sub-populations can be built such that $M < N$, to understand and estimate the considered system dynamics in a simpler manner. However, each sub-population $i \in \{1, \dots, M\}$ in metapopulation modeling is assumed to be well mixed in itself and its recovery rate is homogeneous and constant. Also, the same differential equation can be used to model the spreading within the metapopulation network. Therefore, $p_i(t) \in [0, 1]$ represents the probability of being infected of the subpopulation i , δ_i depicts the recovery rate for the subpopulation i , and the connection between the subpopulation i and j is given as β_{ij} which shows how the node j affects the node i .

Thus, the air transportation network is modeled as a weighted directed graph by using the SIS model dynamics. Airports within the air transport network are considered as nodes of the graph and the edges of the graph represent connections between airports. Each edge is weighted via infection rates which is unique to show the connectivity of two airports by considering the flights between them. Also, there are recovery rates for airports which can be relatable with the capacity usage at airports and has an impact on the delay spreading to die-out. The simple representation of the airport-based metapopulation epidemic process model is as given in the Figure 3.

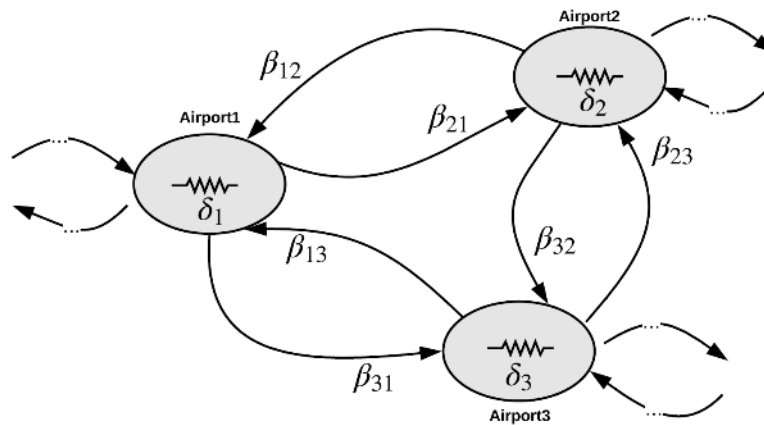


Figure 3: Airport-based metapopulation epidemic process model

In order to find parameters of the delay spreading process of the air traffic metamodel, historical flight-track data of the European air traffic network is used. Additionally, analysis is performed for certain days that involve certain disturbances. Parameters such as infection rates, probability of being infected, recovery rates that will be used in modeling of the epidemic spreading process of the air transport system, are obtained as explained in the following sections.

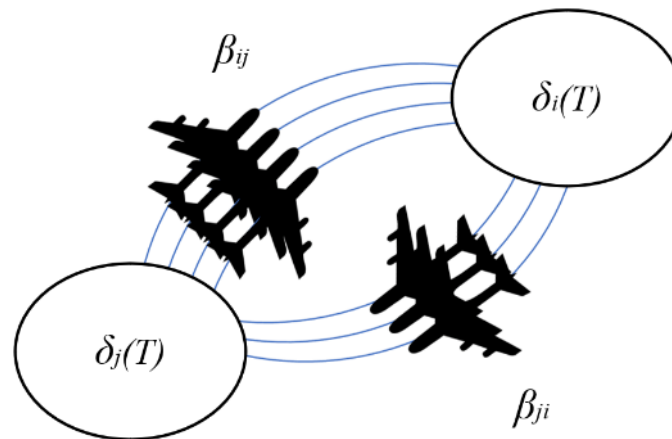


Figure 4: Metamodel representation of the flow between two airports

2.1.1 Determining Infection Rates

Infection rates within the air traffic network is determined by considering the flow rates between airports. β_{ij} represents the infection rate from airport j to airport i . Thus, if there is not any scheduled flight between airport i and airport j in other words if the nodes i and j are not connected, then the infection rate $\beta_{ij} = 0$. It also can be said that $\beta_{ii} = 0$ since airports do not have flights to themselves. To find the normalized directed flow rates between airports for the considered time interval, inflows from different airports are considered.

For generating the infection rates, flight plan data for all the flights within the European air traffic network is used. Specific time interval is selected as one hour. In other saying, inflow flights to airports are observed and normalized for an hour to obtain the infection rates.

2.1.2 Evaluating Probability of Being Infected

In the model, probability of being infected refers to the fraction of the average delay which is observed at the airport for the selected specific time interval (1-hour) that is normalized by the 60-minute delay time which is the maximum value that can be observed for an hour time interval. By obtaining the probability of being infected in that manner, we will be able to capture the state continuity for airports. The probability of being infected is calculated as follows:

$$p_i(t) = \begin{cases} \overline{d_{tw}} / d_{tw(max)}, & \overline{d_{tw}} < d_{tw(max)} \\ 1, & \overline{d_{tw}} \geq d_{tw(max)} \end{cases}$$

where $\overline{d_{tw}}$ is the average delay observed within the specific time window (1-hour for our case) and $d_{tw(max)}$ is the maximum delay accepted that can be observed, which is 60 minutes, within the selected time window. According to the analysis, the average flight duration within the European air traffic network is 132 minutes for January 2018. Additionally, 62 percent of the flight durations are within the 2-hour period and 77 percent of the flights are under 3-hour period. From the network modeling perspective, we have chosen to use updated infection rates which are updated in each 2-hour period.

2.1.3 Evaluating Recovery Rates

Recovery rates for the air traffic network refer to the capacity usage of the airports that provides recovery from a delay for the airport itself and has an impact on the delay spreading within the system. Specifically, one can say that if the recovery rate is low for an airport, it leads to an increase in its delay profiles. Recovery rates for airports are obtained by using the historical flight data. To find those rates, after obtaining the infection rates and probabilities of being infected both at time t and $t + 1$, differential equation for the *SIS* model is solved deterministically as given below:

$$\delta_i = \left(-(p_i(t+1) - p_i(t)) + \sum_{j=1}^N \beta_{ij} p_j(t) (1 - p_i(t)) \right) \frac{1}{p_i(t)}$$

From the operational point of view, it is expected that the recovery rates are roughly same for the airports with similar delay profiles impacted by similar events. Our purpose is to find recovery sets that are not dependent on historical flight data. To overcome this bottleneck, the idea of using deep neural networks for estimation of the recovery rates is introduced in this section. The inputs for this neural network such as capacity of the airport, demand at the airport, total delays and uncertainty of those delays that is observed, disruptive event information that causes a regulation at the airport, etc. are considered. Figure 5 depicts the basic model representation for recovery rate estimation with considered inputs and outputs. $\sum d_i, \sum \sigma_i, C_i, D_i, E_i$ represent the total delay, uncertainty, capacity,

demand, and disruptive event information at airport i , respectively. At the output side, recovery rates and deviation of the uncertainty that is caused by uncertainties at airport i are shown by δ_i and $\delta_{i,\sigma}$.

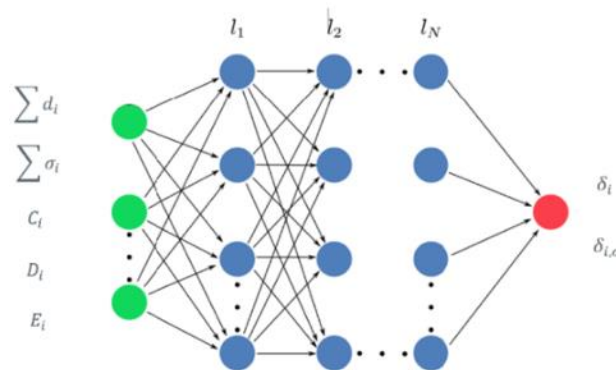


Figure 5: DNN representation of the considered model for estimation of recovery rates

Three examples of the recovery rate estimations of our DNN model are given for different days and time intervals. Figure 6, Figure 7, and Figure 8 depict the recovery rate estimation for June 2, 2018 from 18:00 to 21:00, June 3, 2018 from 13:30 to 16:30, and June 7, 2018 from 14:30 to 17:30, respectively. According to the outputs, the model seems to be performed good enough to use in the airport-based meta-population model. Yet, we observed that the DNN model cannot capture well the less connected airport's recovery rates which does not cause any problem since they do not have a significant impact on the network due to their connection with the other airports, within the selected time interval.

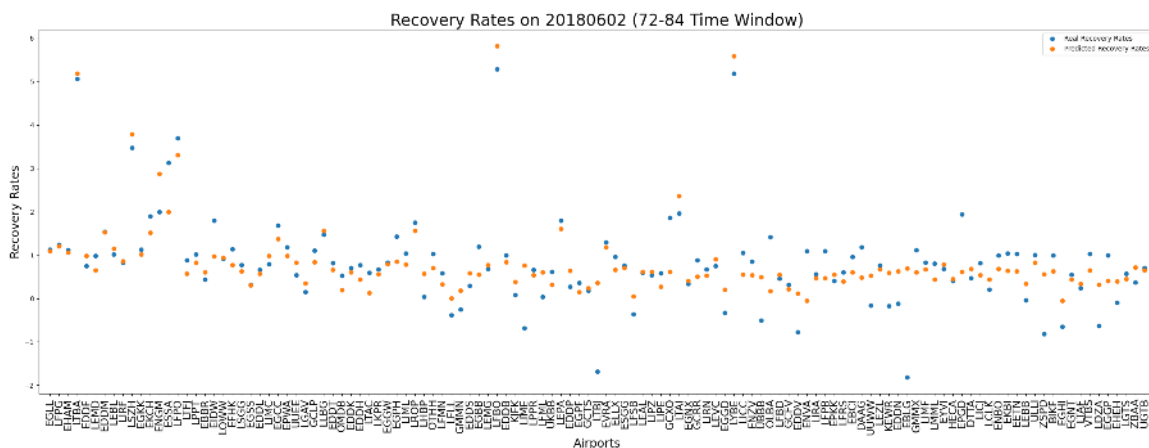


Figure 6: Recovery Rate estimation for June 2, 2018 (18:00 – 21:00)

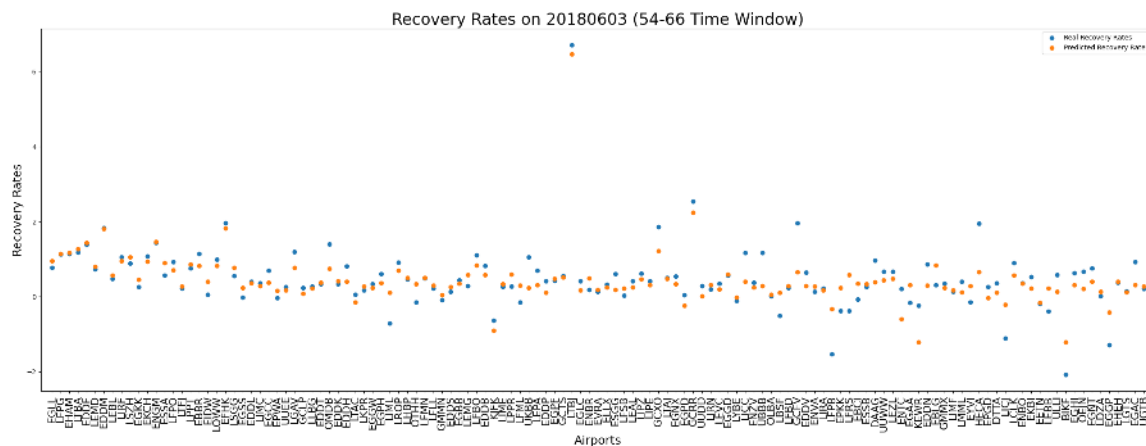


Figure 7: Recovery Rate estimation for June 3, 2018 (13:30 – 16:30)

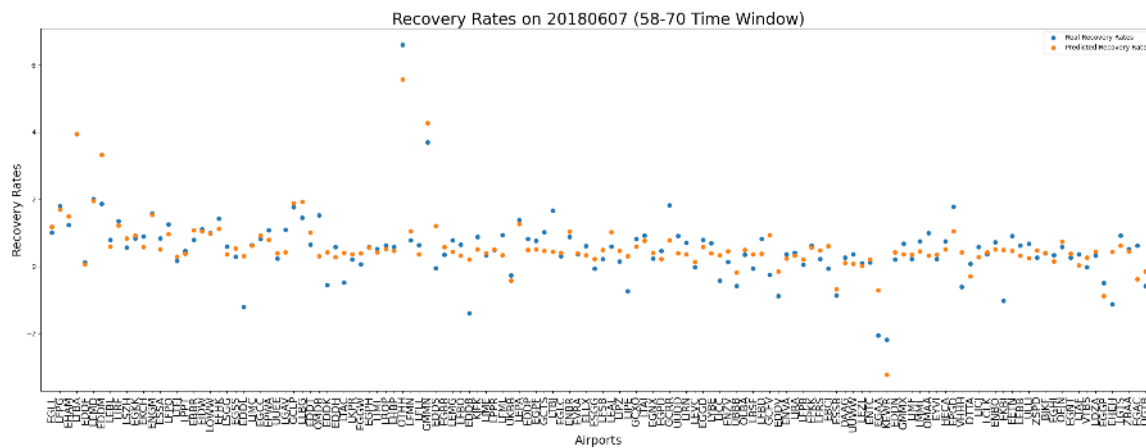


Figure 8: Recovery Rate estimation for June 7, 2018 (14:30 – 17:30)

2.2 Validation Results

In this section, the validation process of our airport-based epidemic network model is given by comparing the results under disruptive events that are found using the model and actual calculations from the flown flights. In this validation study, we have represented the individual trajectory uncertainties with Gaussian distributions and result are depicted over mean values. The data-driven distributions, which are being calculated in WP2 and seen as multivariate Gaussian distributions will be integrated in WP4.

For the model validation, various cases are examined from June 1, 2018 to June 10, 2018. For validation purposes, we are expecting to observe our model outputs to capture the behavior of the airports under disruptive events and approximate the delay trends of the rest of the airports that are operating under their nominal conditions.

Figure 9 shows the comparison between model outputs (on the left) and real fractions (on the right) on June 2, 2018 from 13:30 to 16:30. Selected time window not any disruptive event is applied for he

models. It can be seen that general trends for the airports are able to captured by the model. Real data shows some differentiated activities, e.g., at EEDM and LSZH, not captured well as no any input regarding the cause is applied.

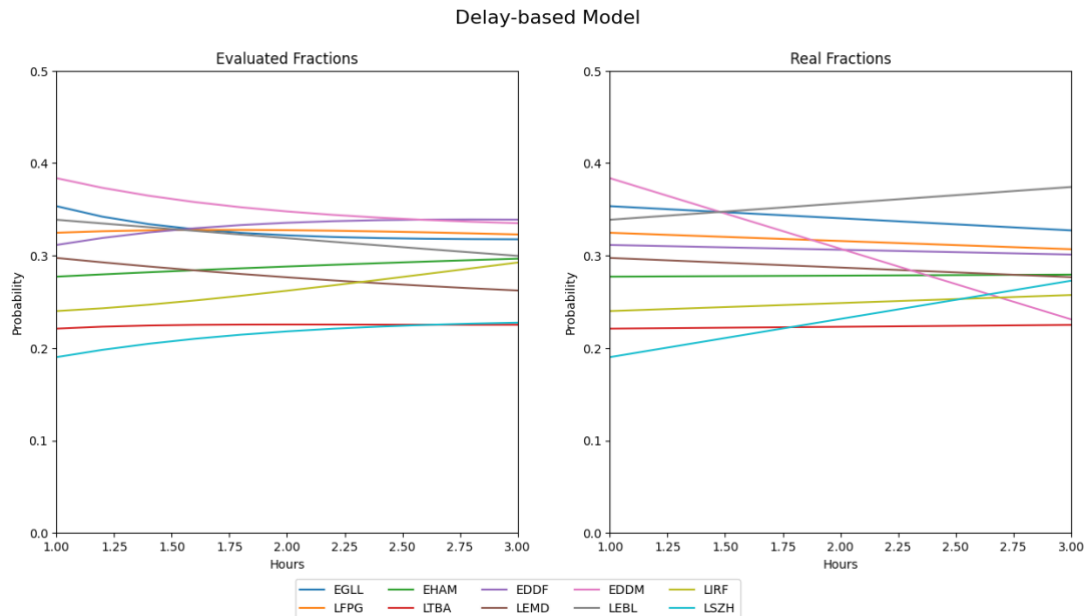


Figure 9: Comparison for evaluated fractions of the model and real fractions on June 2, 2018 (13:30 – 16:30)

In Figure 10, comparison between model outputs (on the left) and real fractions (on the right) on June 2, 2018 from 17:30 to 20:30 is given. A disruptive event at Madrid Barajas Airport (LEMD) is observed within the selected time window. As it can be seen, fraction of being infected of LEMD trend is captured quite well.

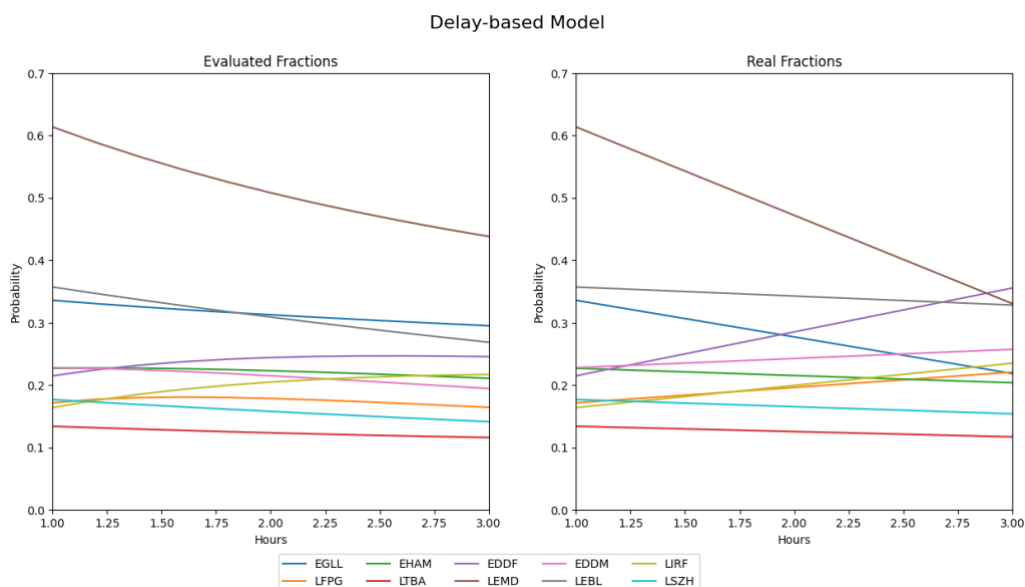


Figure 10: Comparison for evaluated fractions using network model and real fractions on June 2, 2018 (17:30 – 20:30)

In Figure 11, comparison between model outputs (on the left) and real fractions (on the right) on June 3, 2018 from 13:30 to 16:30 is given. A disruptive event at Barcelona El Prat Airport (LEBL) is observed within the selected time window. As it can be seen, fraction of being infected of LEBL trend is fully captured.

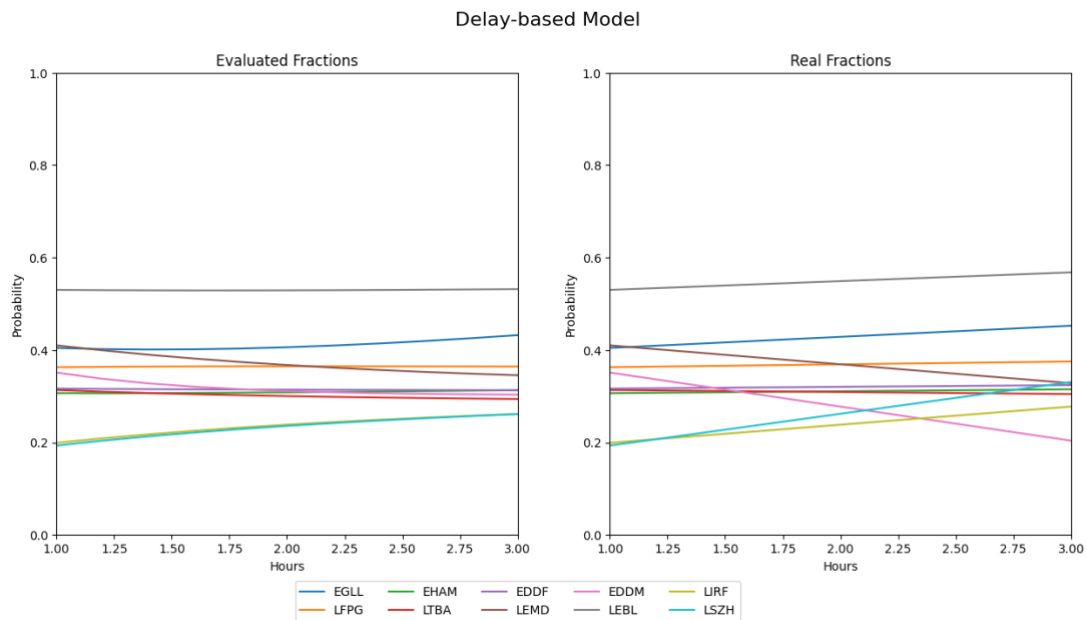


Figure 11: Comparison for evaluated fractions of the model and real fractions on June 3, 2018 (13:30 – 16:30)

In Figure 12, comparison between model outputs (on the left) and real fractions (on the right) on June 6, 2018 from 17:30 to 20:30 is given. Disruptive events at LSZH, LFPG, and Paris Orly Airport (LFPO) are observed within the selected time window such that the model is able to capture the trends.

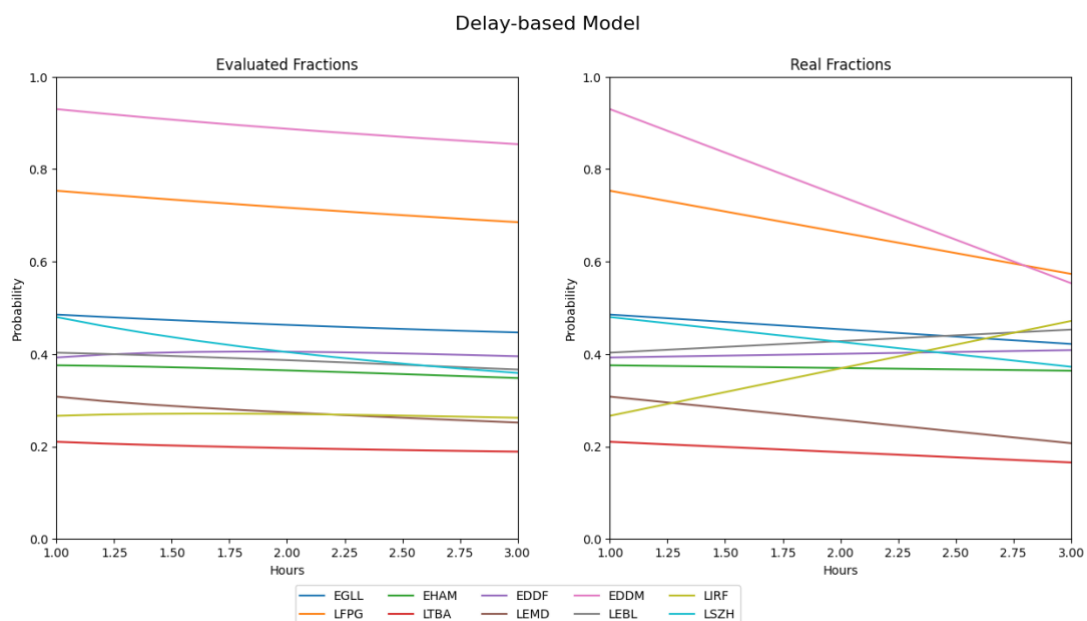


Figure 12: Comparison for evaluated fractions of the model and real fractions on June 6, 2018 (17:30 – 20:30)

In Figure 13, comparison between model outputs (on the left) and real fractions (on the right) on June 8, 2018 from 16:00 to 19:00 is given. Disruptive events at Munich Airport (EDDM) and LSZH are observed within the selected time window. EDDM's and LSZH's being infected probabilities are fully captured. It should be noted that the real data shows a progressing issue at EDDF where the model does not capture as no any input regarding the cause is applied.

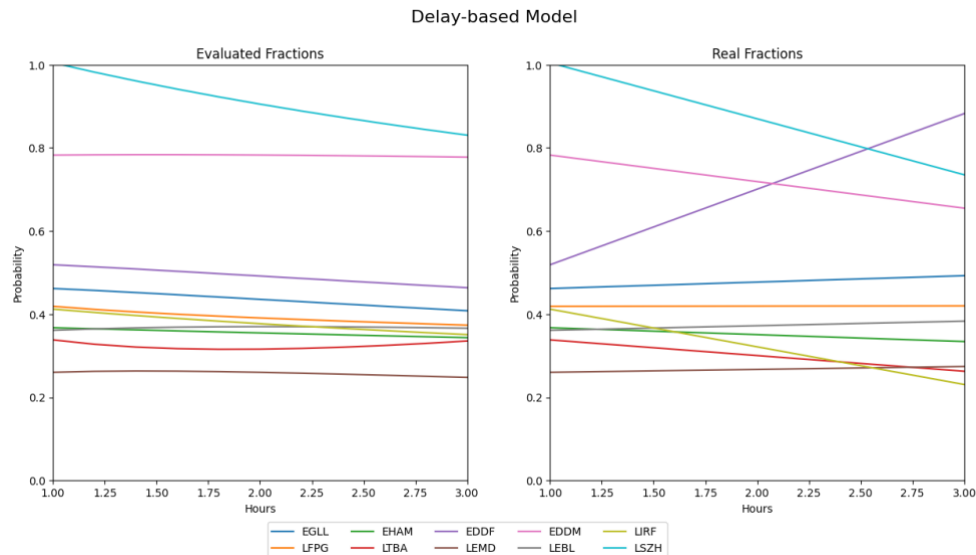


Figure 13: Comparison for evaluated fractions of the model and real fractions on June 8, 2018 (16:00 – 19:00)

In Figure 14, comparison between model outputs (on the left) and real fractions (on the right) on June 8, 2018 from 18:00 to 21:00 is given. Disruptive events at EDDM and LSZH are observed within the selected time window. EDDM's and LSZH's being infected probabilities are captured quite well.

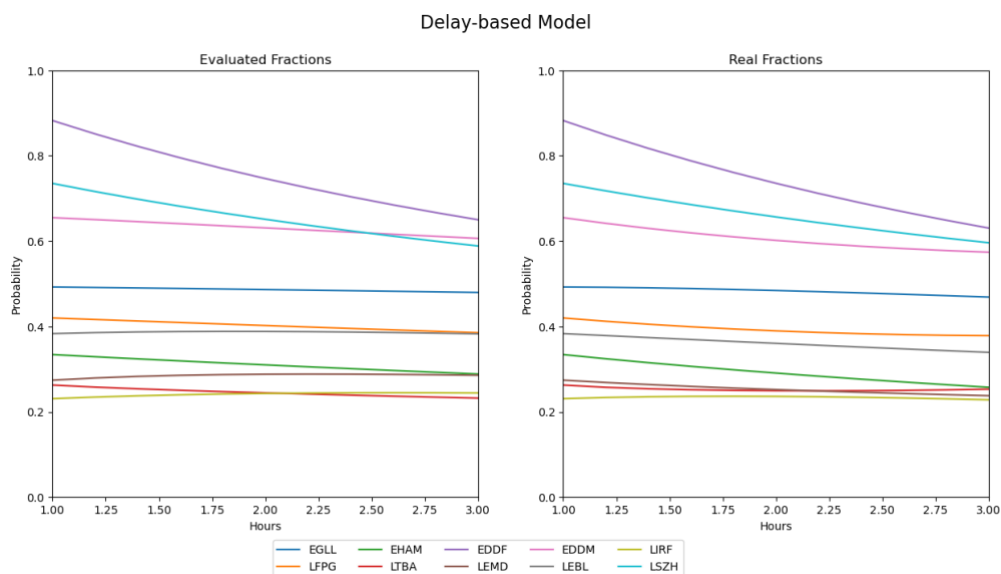


Figure 14: Comparison for evaluated fractions of the model and real fractions on June 8, 2018 (18:00 – 21:00)

In Figure 15, comparison between model outputs (on the left) and real fractions (on the right) on June 9, 2018 from 15:00 to 18:00 is given. Disruptive events at Frankfurt Airport (EDDF), EDDM, Lisbon Portela Airport (LPPT) and LSZH are observed within the selected time window. The response to issue at EEDF is captured by the model quite well.

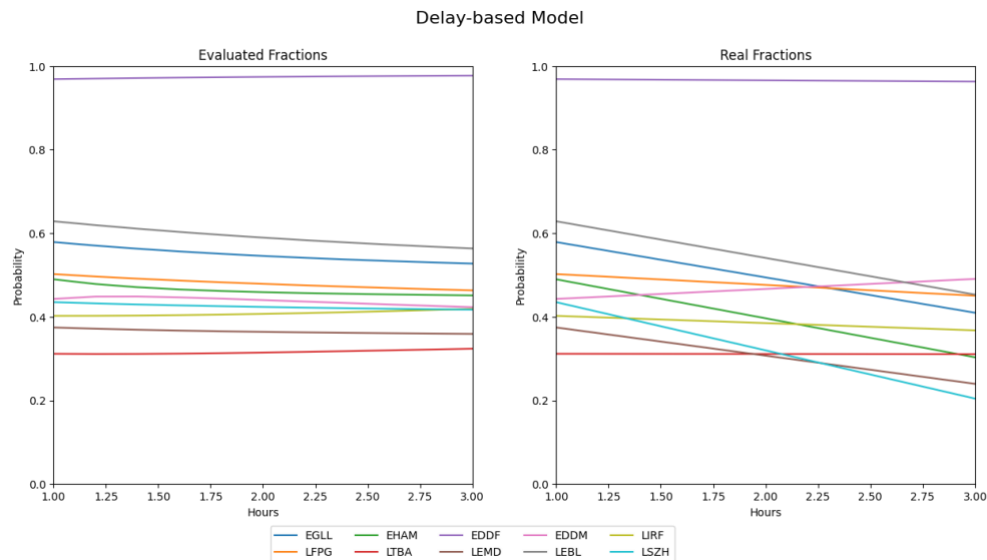


Figure 15: Comparison for evaluated fractions of the model and real fractions on June 9, 2018 (15:00 – 18:00)

In Figure 16, comparison between model outputs (on the left) and real fractions (on the right) on June 9, 2018 from 18:00 to 21:00 is given. Disruptive events at EDDF and LFPG are observed within the selected time window. The response to issues at EEDF and LFPG are captured by the model quite well.

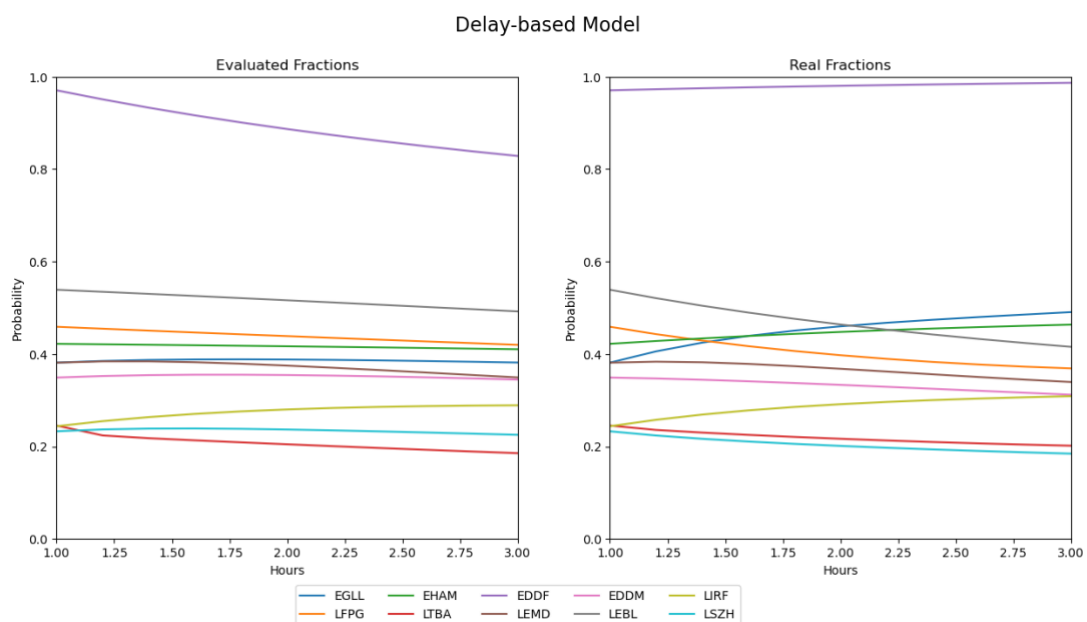


Figure 16: Comparison for evaluated fractions of the model and real fractions on June 9, 2018 (18:00 – 21:00)

3 Network Stability and Resiliency

In the START project, the macro model of ATM is based upon individual trajectories, which carry time-based features and uncertainties. Therefore, each individual trajectory carries uncertainty information comes with the time shift and stochasticity on it as an input to the network model. These uncertainties cause deviations in the arrival and then in departure times, which lead to delay deviations at the airports, consequently, impact the entire network nodes at different rates. Considering the time-based behavior of the system as a whole under disruptive events, one can describe the convergence guarantee through stability theory. In the START Project, we build network resilience upon optimal stability theory, which is well studied by the control theoreticians.

3.1 Network Stability

Consider a set of nonlinear differential equations, which is the model of SIS dynamics, as given in the previous section. Rearranging the equation for a single node in the network as:

$$\dot{p}_i(t) = \sum_{j=1}^N \beta_{ij} p_j(t) - \delta_i p_i(t) - \sum_{j=1}^N \beta_{ij} p_j(t) p_i(t)$$

where $\beta_{ij}, p_i(t), p_j(t) \geq 0$, then $\sum_{j=1}^N \beta_{ij} p_j(t) p_i(t) \geq 0$. It can be written as follows:

$$\begin{aligned} \dot{p}_i(t) &= \sum_{j=1}^N \beta_{ij} p_j(t) - \delta_i p_i(t) - \sum_{j=1}^N \beta_{ij} p_j(t) p_i(t) \\ &\leq \sum_{j=1}^N \beta_{ij} p_j(t) - \delta_i p_i(t) \end{aligned}$$

Therefore, the following linear dynamic system upper-bounds the non-linear dynamical system when they share the same initial conditions under the assumption that outbreak in the linear system will eventually die out, i.e., $\hat{p}(t) \geq p(t)$ for $t \geq 0$ when $\hat{p}(0) = p(0)$.

$$\frac{d\hat{p}_i(t)}{dt} = \sum_{j=1}^N \beta_{ij} \hat{p}_j(t) - \delta_i \hat{p}_i(t)$$

This linear dynamical system can be written in a matrix form as:

$$\frac{d\hat{p}(t)}{dt} = (\mathcal{B} - \mathcal{D})\hat{p}(t)$$

where, $\hat{p}(t) = (\hat{p}_1(t), \hat{p}_2(t), \dots, \hat{p}_M(t))^T$ denotes the state vector of the system, $\mathcal{D} = \text{diag}(\delta_1, \delta_2, \dots, \delta_M)$ denotes the diagonal matrix of recovery rates and $\mathcal{B} = [\beta_{ij}]$ denotes the matrix of infection rates.

The control theory has well written explanation on the stability condition for a system such that all the eigenvalues of $(\mathcal{B} - \mathcal{D})$ must be in the open left half-plane, as seen in Figure 17. Therefore, if the

eigenvalue with largest real part of $(\mathcal{B} - \mathcal{D})$ satisfies $Re[\lambda_{max}(\mathcal{B} - \mathcal{D})] \leq -\alpha$ for some $\alpha > 0$, an initial infection $p(0)$ will converge to zero exponentially fast, i.e., there exists an $\gamma > 0$ such that $\|p_i(t)\| \leq \gamma \|p_i(0)\| e^{-\alpha t}$, for all $t \geq 0$.

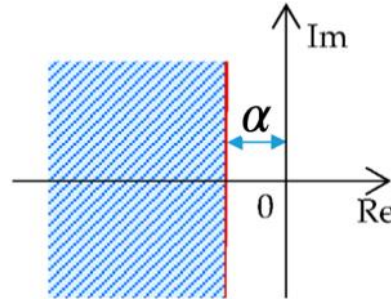


Figure 17. The bounded stability region for system eigenvalues

3.2 ATM Network Resilience

Resilience is defined as an ability of a system to recover quickly from disrupted conditions. From the standpoint of an outbreak in a network (e.g., severe weather impact to an airport), the network resilience is inversely proportional to the die out time of an outbreak. If the outbreak is recovered more quickly, the system can be said: "more resilient" (Gluchshenko & Foerster, 2013).

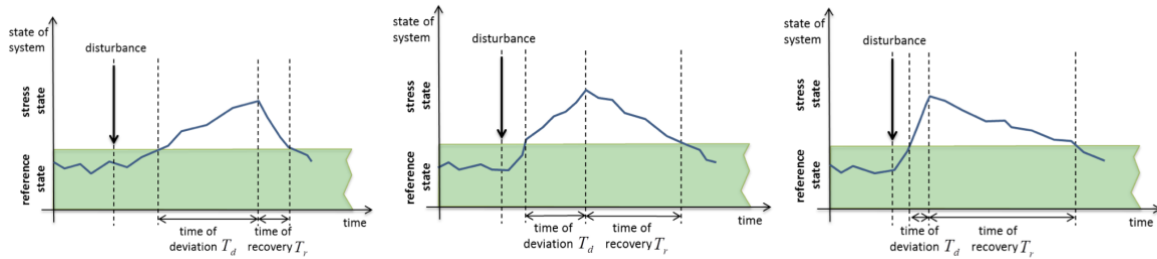


Figure 18. High resilience, mid resilience and low resilience as defined in (Gluchshenko & Foerster, 2013) – depends on settling time value, which can be controlled by $\alpha > 0$ distance, a parameter defines rate of intervene

From ATM Network perspective, EUROCONTROL defines the ability as “the intrinsic ability of a system to adjust its functioning prior to, during, or following changes and disturbances, so that it can sustain required operations under both expected or unexpected condition” (EUROCONTROL, 2009). In our model approach, it has map to prevent the spreading of an outbreak and decrease the die out time with a proper "vaccination" strategy in the epidemic process. From the operational perspective, this strategy corresponds to “actions” of air traffic flow manager such as ground holding, flight cancellation, and airborne holding to balance demand and available capacity. These actions have direct impact over controlling infection rates between airport pairs i.e., $0 \leq \beta_{ij} \leq \bar{\beta}_{ij}$, which can be modified within its feasible intervals through proper management strategy. Specifically, way to make the network more resilient means the more number to apply action to the flights. From operational point of view, the rate of intervention should be upper bounded asymptotically.

At this point, in addition to resilience concept built upon stability, we introduce the "management cost" as an intervention rate can be defined through the function $f_{ij}(\beta_{ij})$ as well. Hence, the maximization of the network resilience with any management strategy can be transformed into an optimization problem:

$$\begin{aligned} & \text{maximize} && \alpha \\ & \text{subject to} && \text{Re}[\lambda_{\max}(\mathcal{B} - \mathcal{D})] \leq -\alpha \\ & && \sum_{i=1}^N \sum_{j=1}^N f_{ij}(\beta_{ij}) \leq T \\ & && \beta_{ij} \leq \beta_{ij} \leq \bar{\beta}_{ij} \quad i, j = 1, \dots, N \end{aligned}$$

where the first constraint is the stability condition, which is explained in the previous subsection. Specifically, the linear dynamical system has an upper bound for the set of non-linear differential equations of the SIS model under the condition that all eigenvalues of the presented linear dynamical system are in the open left half-plane. This strategy is used to minimize the die out time of an outbreak due to disruptive events. The flight cancellation strategy at higher costs, which has higher values especially for airlines, is applicable in addition to the ground holding and airborne holding. Hence the relationship between this "rate of intervention", stability based on $|\alpha|$ distance and reward function is depicted in Figure 19.

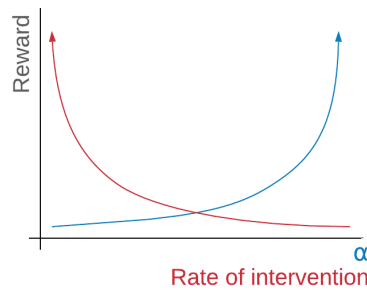


Figure 19. Representation of reward function wrt maximize the stability and minimize the management cost

The second constraint gives T as the total budget that limits the change in infection rates. The total budget T defines the limit of how much intervention is allowed in the whole network. Maximization of α corresponds to the maximization of the system resilience – if α is increased (as seen in Figure 17), the impact dies out faster. The parameter β_{ij} and $\bar{\beta}_{ij}$ are user-defined inputs for the optimization problem, which defines the lower and upper bounds of infection rates.

4 RL-based Network Resilience Management

This section explains the methodology used to solve the introduced optimization-based control problem, a reinforcement learning (RL) approach. RL is a Markov decision process-based method that provides optimal decision making for Markovian problems. Learner or agent in RL problems interacts with a particular environment by taking actions based on its state and observes its outcomes by receiving rewards (or calculating costs) for the agent's actions. This process continues until the agent starts to take optimal actions possible under different conditions, maximizing the agent's total reward and coming up with an optimal policy.

4.1 Proximal Policy Optimization (PPO)

Fundamentally, an agent starts in a state s_t and takes an action a to reach its next state s_{t+1} . Therefore, the probability of transition can be defined as $\Pr(s_{t+1} = s' | s_t = s, a_t = a)$ which defines the transitions as probabilities. Reward function R , on the other hand, represents the rewards that the agent receives for state transitions. Probabilities of transition is updated in each step depending on the rewards collected. Finally, the agent learns a policy π which maximizes the expected cumulative reward where $\pi(a, s) = \Pr(a_t = a | s_t = s)$. We used Proximal Policy Optimization (PPO) algorithm for training our RL agent to provide system resiliency.

PPO algorithm is a policy gradient method that uses the trust region policy optimization (TRPO) advantages such as improving the generalization of the algorithm, which is used for training the RL agents. The details of the PPO algorithm can be found in (Schulman, Wolski, Dhariwal, Radford, & Klimov, 2017). Before starting the training phase of the RL agent, observation space, action space, and reward function have to be defined. Cases for the training process are simply the airport-based meta-population air traffic network model outputs. Training dataset is prepared as from January 2018 to May 2018. From those outputs, cases that can be resilient after optimization are filtered. In other words, cases that the maximum eigenvalue of the system is positive and can become negative after taking the maximum number of actions, are selected as training dataset. Additionally, to include more cases for training dataset, we assumed that the airports that have negative recovery rate, are accepted and expected to have a slight improvement in their operations and increase their recovery rates to 0.1.

For our model the observation space is defined as infection rates which corresponds to the normalized connections between each airport, recovery rates of the airports, and real part of maximum eigenvalue of the system which allows us to tell if the system is stable/resilient or not. Therefore, the observation space can be represented as $\Omega = \{ \mathcal{B}, \mathcal{D}, \text{Re}[\lambda_{\max}(\mathcal{B} - \mathcal{D})] \}$.

Action space, on the other hand, is defined as changing the infection rates. RL agent is modelled to give the percentage change in the infection rates which answers the question what is the percentage of the flights has to be intervened. After the agent generates actions for each OD pair in the network, those values are used to calculate the new maximum eigenvalue of the system to see if the system become resilient. Action space is limited as $0.5 * \beta \leq \hat{\beta} \leq 1 * \beta$, which means for each OD pair maximum number of flights that can be intervened by the agent is 50% of the total flights between OD pairs within the selected time interval.

Lastly, reward functions are considered from two perspectives that are the maximum eigenvalue of the system and the number of actions taken. Since providing the system stability is the main goal for

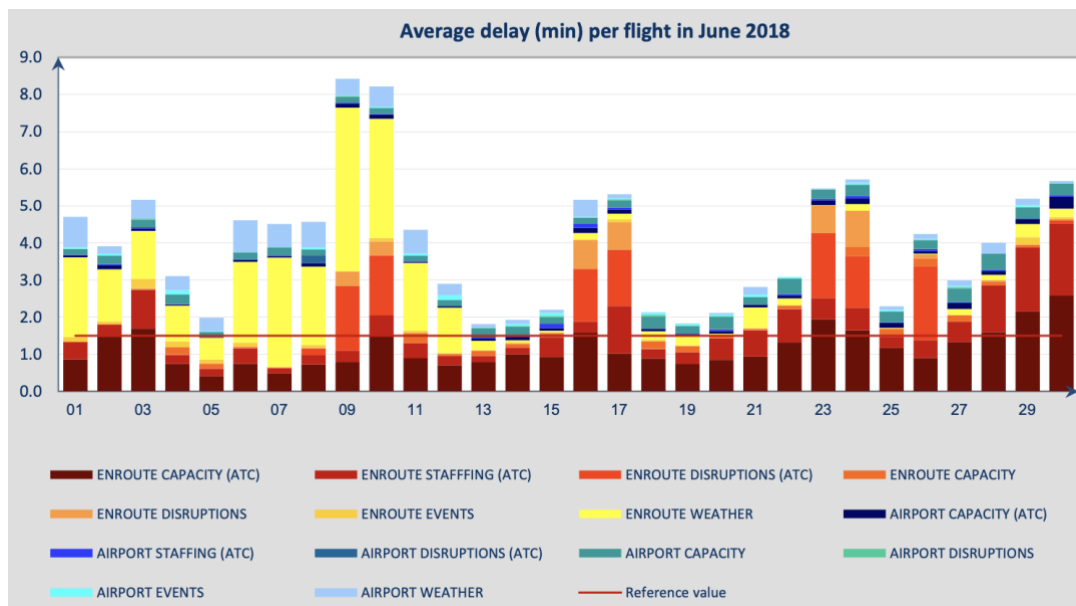
us, if the real part of the system's maximum eigenvalue becomes negative then the agent starts to receive positive rewards. Yet, considering the costs of the operational actions in air traffic management such as ground holdings and flight cancellations, the agent needs to ensure the resiliency with minimum number of actions possible. Therefore, we decided to use the following reward function while we consider the maximum eigenvalue-based approach:

$$R_{eig} = \exp(k * Re[\lambda_{max}(\mathcal{B} - \mathcal{D})])$$

where the agent increases its reward exponentially by making the real part of the maximum eigenvalue of the system close to zero but negative. The importance of being close to 0 is enhanced with parameter k which is a scalar value. If the maximum eigenvalue stays in the positive side, agent receives a big penalty which ends up with a negative reward at the end of the episode. For the number of taken actions perspective, on the other hand, we wanted to ensure that each action within the system is a useful action to make the system stable. Thus, to prevent the agent to take unnecessary actions that do not have an impact on the system stability, we defined a penalty function which gives negative rewards for each action taken. Finally, we used the weighted combination of those reward functions for the training process of the RL agent.

4.2 Results of Resilience Management under Disruptive Events

In this subsection, results that are obtained after resiliency management through the RL-based methodology are shown. In addition to this, we show differences between RL solutions of different models that are trained with only eigenvalue-based reward function and the combination of eigenvalue-based and action-based reward functions. The difference comes from the models trained for high resiliency, which means only counts system stability and quick recovery; and trained for balanced action considers system stability and intervention (operational) cost, respectively. To provide results, we present three example cases obtained from original data on June 4, 9 and 10 in 2018, where thunderstorms affected large areas of North West Europe with intense local convective activity. The following plots are taken from EUROCONTROL's Monthly Network Operation Report of June 2018 to show these disruptive effects.



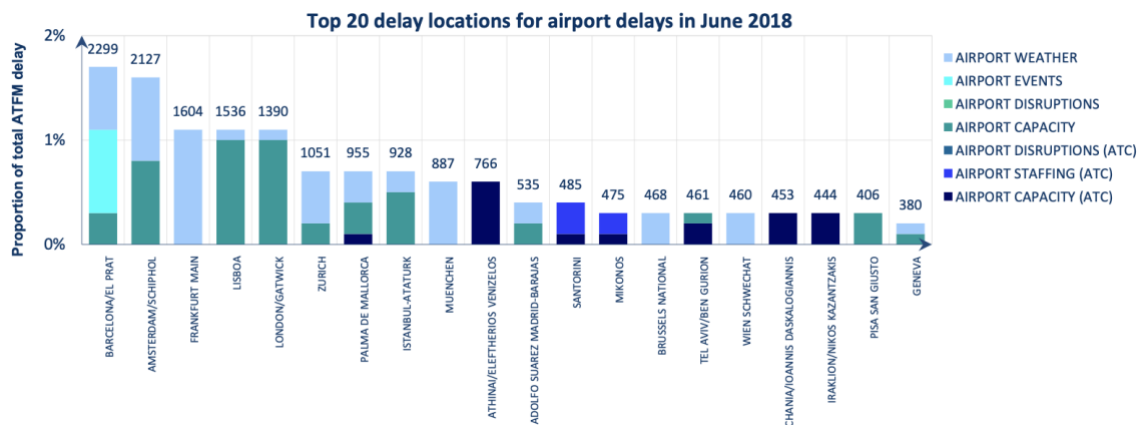


Figure 20. Observed disruptive events over North-West Europe in June 2018 as see in EUROCONTROL's Monthly Network Operation Report

4.2.1 Case Study #1 – Convective Activity over Zurich Airport

Figure 21 depicts the comparison between evaluated fractions before and after providing the system stability on June 4, 2018 from 13:30 to 16:30. In that case, there is a disruptive event observed at LSZH within the selected time interval. Before maximizing the system resilience, the real part of the system's maximum eigenvalue was $Re[\lambda_{max}(\mathcal{B} - \mathcal{D}I)] = 0.0384$, which is positive and makes the system unstable. After the resilience management with constraint on intervention rate, we observed that the maximum eigenvalue became negative ($Re[\lambda_{max}(\mathcal{B} - \mathcal{D}I)] = -0.0209$) which means the system stability is improved significantly. Figure 21 - b, shows the resilience management result without penalties for the number of actions taken (high resilience case). We observed that the system resilience can be ensured quicker, yet, unnecessary actions are taken which have a high impact in terms of operational costs. As a result, Figure 21, shows decrease in the fractions of the busiest 10 airports that have flights from LSZH within that time interval, which are EDDF, EGLL, LEMD, and LTBA. Table 4 shows the previous and new infection rates and percentage changes of the flights from LSZH to those airports.

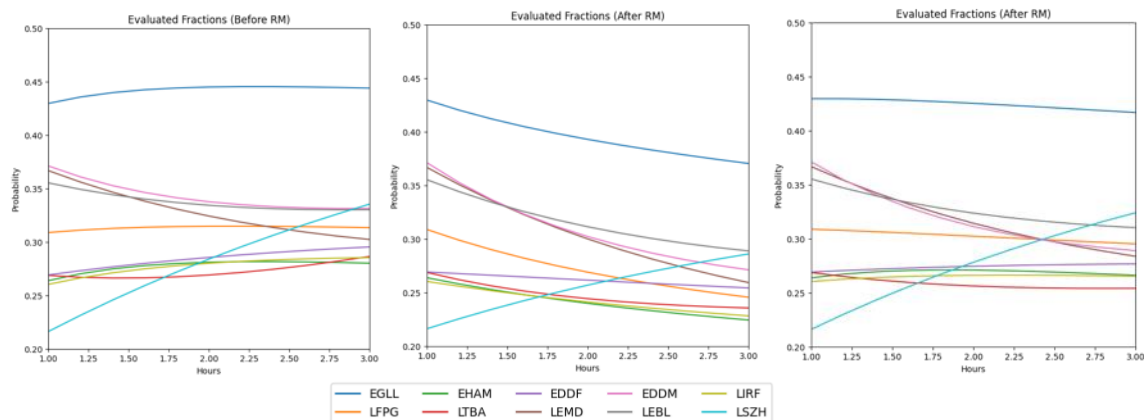


Figure 21: Comparison between evaluated fractions a) without resilience management and b) after resilience management without constraint on rate of intervention (high resilience), and c) after resilience management with constraint on rate of intervention for June 4, 2018 (13:30 – 16:30)

Table 4: Infection rate changes of the flights from LSZH to the some of the major airports that have connection (June 4, 2018 - 13:30 – 16:30) after applying resilience management with constraint on rate of intervention

	LSZH June 4, 2018 13:30-16:30		
	β_{old}	β_{new}	# of Intervened Flights
EGLL	0,021277	0,020851	0
LTBA	0,029412	0,022941	1
EDDF	0,021739	0,020217	0
LEMD	0,036364	0,024364	1

Table 5: Calculated minutes of delays (total and per flight) with and without resilience management (RM) from LSZH to the some of the major airports that have connection (June 4, 2018 - 13:30 – 16:30)

	June 4, 2018 – 13:30-16:30				
	avg Delay per Flight (minutes) before RM	avg Delay per Flight (minutes) after RM	Total Delay (minutes) before RM	Total Delay (minutes) after RM	Delta Delay (minutes) per Flight
EGLL	26,62	25,20	2076,11	1965,70	-1,42
LFPG	18,80	17,74	1240,63	1170,92	-1,06
EHAM	16,80	16,14	1176,04	1129,96	-0,66
LTBA	16,02	14,66	1025,57	938,04	-1,37
EDDF	17,71	16,35	1098,25	1013,70	-1,36
LEMD	17,98	16,87	970,71	911,13	-1,10
EDDM	19,64	17,89	1767,80	1609,83	-1,76
LEBL	19,56	18,87	1075,61	1037,70	-0,69
LIRF	17,12	16,10	873,34	821,24	-1,02
LSZH	20,11	18,76	965,47	900,59	-1,35

4.2.2 Case Study #2 – Thunderstorm over Frankfurt and Barcelona Airport

Figure 22 shows the comparison between evaluated fractions before and after providing the system resilience on June 7, 2018 from 12:30 to 15:30. In that case, disruptive events are observed at EDDF

and LEBL within the selected time interval. Before maximizing the system resilience, the real part of the system's maximum eigenvalue was $Re[\lambda_{max}(\mathcal{B} - DI)] = 0.0048$, which is positive and makes the system unstable. After the resilience management, we observed that the maximum eigenvalue became negative ($Re[\lambda_{max}(\mathcal{B} - DI)] = -0.0358$) which means the system stability is improved. Figure 22 - b shows the resilience management results for without penalties for the number of actions. It can be seen that the system stability can be ensured again but also unnecessary actions are taken which increases operational costs. In Figure 22, as expected, it is seen decrease in the fractions of the busiest 10 airports that have flights from EDDF and LEBL within that time interval. For EDDF those airports are EGLL, LFPG, EHAM, LTBA, LEMD, and LIRF; for LEBL those airports are EGLL, LFPG, EHAM, and LEMD. Table 6 and Table 7 shows the previous and new infection rates and percentage changes of the flights from EDMM and EDDF to the corresponding airports, respectively.

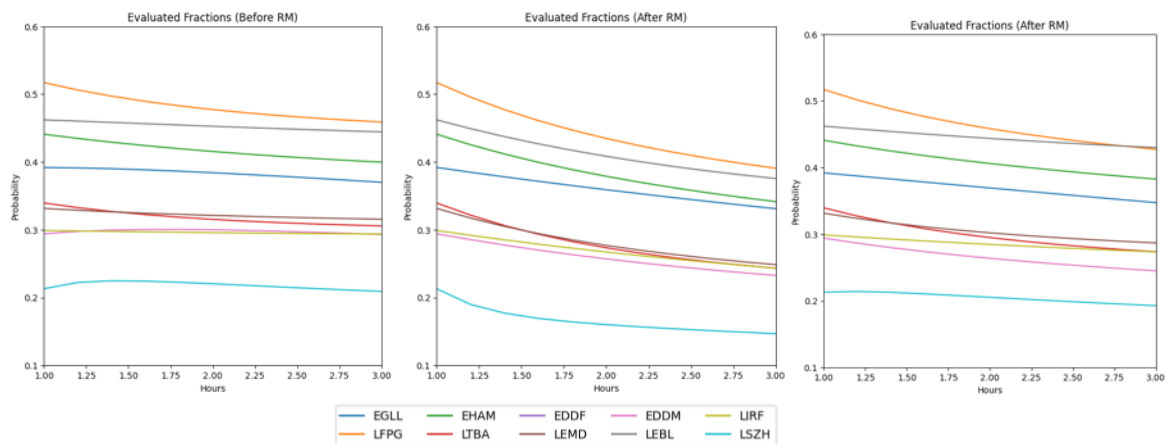


Figure 22: Comparison between evaluated fractions a) without resilience management and b) after resilience management without constraint on rate of intervention (high resilience), and c) after resilience management with constraint on rate of intervention for June 7, 2018 (12:30 – 15:30)

Table 6: Infection rate changes of the flights from EDDF to the some of the major airports that have connection (June 7, 2018 - 12:30 – 15:30) after applying resilience management with constraint on rate of intervention

	LEBL June 7, 2018 12:30-15:30		
	β_{old}	β_{new}	# of Intervened Flights
EGLL	0,023256	0,019070	0
LFPG	0,022222	0,020889	0
EHAM	0,020000	0,016000	1
LEMD	0,050000	0,039500	1

Table 7: Infection rate changes of the flights from LEBL to the some of the major airports that have connection (June 7, 2018 - 12:30 – 15:30) after applying resilience management with constraint on rate of intervention

	EDDF June 7, 2018 12:30-15:30		
	β_{old}	β_{new}	# of Intervened Flights
EGLL	0,023256	0,012093	1
LFPG	0,044444	0,033778	0
EHAM	0,020000	0,010200	1
LTBA	0,026316	0,017632	1
LEMD	0,025000	0,017750	0
LIRF	0,034483	0,028966	0

Table 8: Calculated minutes of delays (total and per flight) with and without resilience management (RM) from EDDF and LEBL to the some of the major airports that have connection (June 7, 2018 - 12:30 – 15:30)

	June 7, 2018 – 12:30-15:30				
	avg Delay per Flight (minutes) before RM	avg Delay per Flight (minutes) after RM	Total Delay (minutes) before RM	Total Delay (minutes) after RM	Delta Delay (minutes) per Flight
EGLL	22,21	20,94	1665,39	1570,41	-1,27
LFPG	27,54	25,73	2037,94	1903,82	-1,81
EHAM	23,98	22,44	2206,62	2064,56	-1,54
LTBA	18,35	16,82	1100,95	1009,19	-1,53
EDDF	60,00	55,53	2880,00	2665,62	-4,47
LEMD	18,93	17,08	1117,09	1007,78	-1,85
EDDM	17,59	15,16	879,29	757,88	-2,43
LEBL	26,67	25,67	1333,38	1283,31	-1,00
LIRF	17,63	16,41	916,68	853,58	-1,21
LSZH	12,54	11,37	714,97	648,23	-1,17

4.2.3 Case Study #3 – Continuing Thunderstorm over Frankfurt and Munich Airport

Figure 23 depicts the comparison between evaluated fractions before (on the right) and after (on the left) providing the system resilience on June 10, 2018 from 13:00 to 16:00. In that case, disruptive events are observed at EDDM and EDDF within the selected time interval. Before maximizing the system resilience, the real part of the system's maximum eigenvalue was $Re[\lambda_{max}(\mathcal{B} - \mathcal{D}I)] = 0.0409$, which is positive and makes the system unstable. After the resilience management, we observed that the maximum eigenvalue became negative ($Re[\lambda_{max}(\mathcal{B} - \mathcal{D}I)] = -0.0071$) which means the system stability is improved. Figure 23-b, depicts the resilience management results for without the number of actions penalties. We observed that the system stability can be ensured with high damping, however, unnecessary actions are taken, which causes an increment in operational costs. In summary, in Figure 23, we see decrease in the fractions of the busiest 10 airports that have flights from EDDM and EDDF within that time interval. For EDDM those airports are EHAM, LEMD, LEBL, LIRF, and LSZH; for EDDF those airports are EGLL, LFPG, EHAM, LEMD, EDDM, and LEBL. Table 9 and Table 10 shows the previous and new infection rates and percentage changes of the flights from EDMM and EDDF to the corresponding airports, respectively.

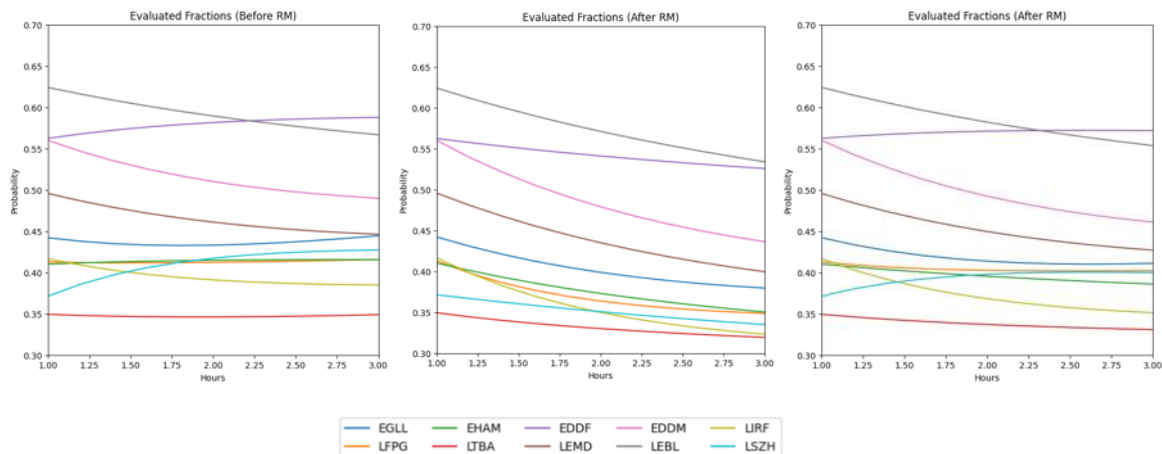


Figure 23: Comparison between evaluated fractions a) without resilience management and b) after resilience management without constraint on rate of intervention (high resilience), and c) after resilience management with constraint on rate of intervention for June 10, 2018 (13:00 – 16:00)

Table 9: Infection rate changes of the flights from EDDM to the some of the major airports that have connection (June 10, 2018 - 13:00 – 16:00) after applying resilience management with constraint on rate of intervention

	EDDM June 10, 2018 13:00-16:00		
	β_{old}	β_{new}	# of Intervened Flights
EHAM	0,026316	0,023421	0
LEMD	0,020408	0,019796	0
LEBL	0,032258	0,020323	1
LIRF	0,027778	0,015000	1
LSZH	0,062500	0,038750	1

Table 10: Infection rate changes of the flights from EDDF to the some of the major airports that have connection (June 10, 2018 - 13:00 – 16:00) after applying resilience management with constraint on rate of intervention

	EDDF June 10, 2018 13:00-16:00		
	β_{old}	β_{new}	# of Intervened Flights
EGLL	0,022222	0,013111	1
LFPG	0,027027	0,017838	1
EHAM	0,026316	0,015000	1
LEMD	0,040816	0,031429	0
EDDM	0,017857	0,017500	0
LEBL	0,032258	0,017097	1

Table 11: Calculated minutes of delays (total and per flight) with and without resilience management (RM) from EDDM and EDDF to the some of the major airports that have connection (June 10, 2018 - 13:00 – 16:00)

June 10, 2018 – 13:00-16:00					
	avg Delay per Flight (minutes) before RM	avg Delay per Flight (minutes) after RM	Total Delay (minutes) before RM	Total Delay (minutes) after RM	Delta Delay (minutes) per Flight
EGLL	26,68	24,13	2214,57	2002,49	-2,56
LFPG	24,96	23,96	1846,85	1773,00	-1,00
EHAM	24,95	23,65	1896,34	1797,36	-1,30
LTBA	20,96	19,17	1341,33	1227,01	-1,79
EDDF	35,27	34,60	2539,79	2491,23	-0,67
LEMD	26,79	25,17	1125,20	1057,20	-1,62
EDDM	29,40	27,56	1558,32	1460,61	-1,84
LEBL	34,01	33,16	1530,60	1492,02	-0,86
LIRF	23,11	21,99	1178,66	1121,55	-1,12
LSZH	25,65	23,69	1590,50	1468,58	-1,97

Finally, Table 5, Table 8 and Table 11 provides the calculated delays for per flight (average) and total flight delay in the major airports have connection between the airports impacted by disruptive events. As it can be seen from the tables, resilience management provides effective reduction in delay, while keeping intervention rate low.

5 Concluding Remarks

In this deliverable, we have explained the management methodology of the ATM macro model, enabling us to choose the best actions to ensure the resiliency of the network under disruptive events. First, we gave the resiliency definition, and then it has been connected with the theory of network stability, which is well defined and well-studied. From the operational point of view, resiliency is also associated with the management cost as a function of the intervention rate; hence the "resiliency" has been given through binding with recovery time. This is quite similar to fitting "settling time," defined as "time for washing away the effect of the transition period when one disturbed the system." The problem, at this point, transformed into an optimization-based stability problem to guarantee convergence by time, meaning the effect of disruptive events dies out eventually. Quick recovery is typically preferred, but in this case, it applies significant intervention measures impacting many flights. Considering this trade-off, finally, we transformed the problem into an optimization problem and solved it through reinforcement learning (RL) methodology. RL provided us to choose the target OD pair, and the number of flights requires regulation action. The case studies and results are given for the selected time windows chosen in the interval of 1-10 June of 2018, where thunderstorms affected large areas of North-West Europe with intense local convective activities.

The results have been given by applying the regulation generated by the algorithm, which is developed in WP3 of START. It is observed that high resilience measures without constraint over intervention rate and low resilience measures considering management cost show quite different trends, as expected. This comes from setting the "settling time" of the response to the disturbances -- this is a pretty well-known phenomenon from linear control theory. It is obvious that one can choose the weights according to the actual costs for issuing greedy regulation or providing soft management, high resiliency, and low resiliency, respectively. In WP4, the START project considers regulations over trajectories with different operational costs as well, and the further integration with macro-level management, which is given in this deliverable, will put another dimension into the problem. The integrated results will be provided through the outcomes of WP4.

6 References







- Frolow, I., & Sinnott, J. (1989). National airspace system demand and capacity modeling. *Proceedings of the IEEE*, 77(11), 1618-1624.
- Wieland, F. (1997). Limits to growth: results from the detailed policy assessment tool [air traffic congestion]. *16th DASC. AIAA/IEEE Digital Avionics*. 2. IEEE.
- Bilimoria, K., Sridhar, B., Chatterji, G., Sheth, K., & Grabbe, S. (2001). FACET: Future ATM concepts evaluation tool. *Air Traffic Control Quarterly*, 9(1), 1-20.
- Long, D., Lee, D., Johnson, J., Gaier, E., & Kostiuk, P. (1999). *Modeling air traffic management technologies with a queuing network model of the national airspace system*. National Aeronautics and Space Administration, Langley Research Center.
- Long, D., & Hasan, S. (2009). Improved predictions of flight delays using LMINET2 system-wide simulation model. *9th AIAA Aviation Technology, Integration, and Operations Conference (ATIO)*. Hilton Head, SC.
- Pyrgiotis, N., Malone, K., & Odoni, A. (2013). Modelling delay propagation within an airport network. *Transportation Research Part C: Emerging Technologies*, 27, 60–75.
- Baspinar, B., Ure, N., Koyuncu, E., & Inalhan, G. (2016). Analysis of delay characteristics of European air traffic through a data-driven airport-centric queuing network model. *14th IFAC Symposium on Control in Transportation Systems*. Istanbul.
- Bapinar, B., Koyuncu, E., & Inalhan, G. (2017). Large scale data-driven delay distribution models of European air traffic. *Transportation research procedia*, 22, 499-508.
- Baspinar, B., & Koyuncu, E. (2016). A data-driven air transportation delay propagation model using epidemic process models. *International Journal of Aerospace Engineering*, 2016.
- Dietz, K., & Heesterbeek, J. (2002). Daniel Bernoulli's epidemiological model revisited. *Mathematical bio-sciences*, 180(1), 1-21.
- Kermack, W., & McKendrick, A. (1927). A contribution to the mathematical theory of epidemics. *Proceedings of the Royal Society of London A: mathematical, physical and engineering sciences*, 115(772), 700-721.
- Zhou, Y., & Liu, H. (2003). Stability of periodic solutions for an SIS model with pulse vaccination. *Mathematical and Computer Modelling*, 38(3), 299-308.
- Nowzari, C., Preciado, V., & Pappas, G. (2016). Analysis and control of epidemics: a survey of spreading processes on complex networks. *Control Systems, IEEE*, 36(1), 26-46.
- Hethcote, H. (1989). Three basic epidemiological models. *Applied mathematical ecology*, 119-144.
- Li, C., van de Bovenkamp, R., & Van Mieghem, P. (2012). Susceptible-infected-susceptible model: a comparison of n-intertwined and heterogeneous mean-. *Physical Review E*, 86(2).

- Lajmanovich, A., & Yorke, J. (1976). A deterministic model for gonorrhea in a nonhomogeneous population. *Mathematical Biosciences*, 28(3), 221-236.
- Romualdo, P., & Alessandro, V. (2001). Epidemic spreading in scale-free networks. *Physical review letters*, 86(14), 3200.
- Balcan, D., Colizza, V., Goncalves, B., Hu, H., Ramasco, J., & Alessandro, V. (2009). Multiscale mobility networks and the spatial spreading of infectious diseases. *Proceedings of the National Academy of Sciences*, 106(51), 21484-21489.
- Capasso, V., & Capasso, V. (1993). *Mathematical structures of epidemic systems*. Springer.
- Hethcote, H. (2000). The mathematics of infectious diseases. *SIAM review*, 42(4), 599-653.
- SESAR Exploratory Research. (2020). *Project Management Plan, D1.1 START*. H2020-SESAR-2019-2.
- Schulman, J., Wolski, F., Dhariwal, P., Radford, A., & Klimov, O. (2017). Proximal policy optimization algorithms. *arXiv preprint arXiv:1707.06347*.
- EUROCONTROL. (2009). *A white paper on resilience engineering for ATM*. Retrieved from <https://www.eurocontrol.int/sites/default/files/2019-07/white-paper-resilience-2009.pdf>
- Gluchshenko, O., & Foerster, P. (2013). Performance based approach to investigate resilience and robustness of an ATM System. *Tenth USA/Europe Air Traffic Management Research and Development Seminar*. Chicago.



FL/GHTKEY



Participant No		Participant organisation name	Country
1 - BRTE		Boeing Research and Technology Germany (BRTE)	Germany
2 - DLR		German Aerospace Center (DLR)	Germany
3- ENAC		Ecole Nationale de l'Aviation Civile (ENAC)	France
4- FK	FL/GHTKEY	FlightKeys (FK)	Austria
5- ITU		Istanbul Teknik Universitesi (ITU)	Turkey
6 – UC3M (Coordinator)	 Universidad Carlos III de Madrid	Universidad Carlos III de Madrid (UC3M)	Spain
7 - UPC	 UNIVERSITAT POLITÈCNICA DE CATALUNYA BARCELONATECH	Universitat Politècnica de Catalunya (UPC)	Spain